Korean Journal of Remote Sensing, Vol.35, No.4, 2019, pp.491~502
https://doi.org/10.7780/kjrs.2019.35.4.1
ISSN 1225-6161 (Print)
ISSN 2287-9307 (Online)

Article

Glacier Change in the Yigong Zangbo Basin, Tibetan Plateau, China

Chang-Qing Ke [1)†] · Hoonyol Lee [2)] · Yan-Fei Han [3)]

Abstract: Distinguishing debris-covered glaciers from debris-free glaciers is difficult when using only optical remote sensing images to extract glacier boundaries. According to the features that the surface temperature of debris-covered glacier is lower than surrounding objects, and higher than clean glaciers, glacial changes in the Yigong Zangbo basin was analyzed on the basis of visible, near-infrared and thermal-infrared band images of Landsat TM and OLI/TIRS in the support of ancillary digital elevation model (DEM). The results indicated that glacier area gradually declined from 928.76 km^2 in 1990 to 918.46 km^2 in 2000 and 901.51 km^2 in 2015. However, debris-covered glacier area showed a slight increase from 63.39 km^2 in 1990 to 66.24 km^2 in 2000 and 71.16 km^2 in 2015. During 25 years, the glacier length became shorter continuously with terminus elevation rising up. The area of moraine lakes in 1990 was 1.43 km^2, which increased to 1.98 km^2 in 2000 and 3.41 km^2 in 2015. In other words, the total area of the moraine lakes in 2015 is 2.38 times of that in 1990. This increase in moraine lake area could be the result of accelerated glacier melt and retreat, which is consistent with the significant warming trend in recent decades in the basin.

Key Words: Thermal Infrared Remote Sensing, Debris-covered Glacier, Moraine Lake, Air Temperature Rise, Yigong Zangbo Basin

1. Introduction

The cryosphere is one of the main factors that affect changes in global sea level. Alpine glaciers are the most sensitive to climate change and are used as indicator for climate change (Zhou *et al*., 2018). Glacier retreat is accelerating with global warming as the amounts of CO_2 and other greenhouse gases increase. To obtain information regarding the distribution and changing trends of glaciers, glacier inventory programs have been launched by the National Snow and Ice Data Center (NSIDC), the World Data Center in Cambridge (WDC-C) for Glaciology, the National Oceanic and Atmospheric Administration (NOAA), the National

Received April 2, 2019; Revised April 24, 2019; Accepted May 21, 2019; Published online August 6, 2019

1) Professor, School of Geography and Ocean Science, Nanjing University
2) Professor, Department of Geophysics, Kangwon National University
3) Master Student, School of Geography and Ocean Science, Nanjing University

† Corresponding Author: Chang-Qing Ke (kecq@nju.edu.cn)

Aeronautics and Space Administration (NASA) and other agencies (Li *et al*., 1999). There are over 36,000 glaciers in the western China, only a few of them are under long-term observations (Shi and Liu, 2000). Glacier No. 1 in Tianshan, the headwater of Urumqi River, is the only one with nearly 30 years of observation data (Liu *et al*., 1999). Chinese Glacier Inventory (CGI) was built over 20 years and completed in 1999. This inventory mainly reflects the status of glaciers during the first aerial mapping period (late 1950s to late 1970s) in China and is a comprehensive collection of aerial photographs, topographic maps and field survey data for individual glaciers and for China's basic glacier data census (Liu *et al*., 2000). However, the CGI does not reflect present status of glacier changes.

With the development of satellite imaging technology, remote sensing images can be used to identify glaciers for real-time, dynamic and large-scale monitoring. Remote sensing technology can be used to monitor alpine glaciers that have no field survey data. Thus, it can be used to properly evaluate and predict glacier changes and to analyze the impacts of the observed glacier changes on water resource and river runoff in arid areas in western China. In addition, it provides basic information on the use of water resources and ecological environmental protection. Traditional glacier identification methods include the use of threshold statistics, the ratio method, the Normalized Difference Snow Index (NDSI) method, and so on (Yan and Wang, 2013). Shangguan *et al*. (2004) used the NDSI to extract glacier information of headwater region of the Yulongkashi River for examining the glacial changes. However, those methods are unable to distinguish debris-covered glacier, which has an area of 26,000 km^2 at a global scale (Scherler *et al*., 2018). The presence of debris can not only reduce glacier ablation, but also strongly alters the surface boundary condition and thus heat exchanges with the atmosphere (Collier *et al*., 2015).

Generally, the terminus of a glacier in the western China is covered by a layer of debris (Shi and Liu, 2000). The spectral characteristics of glaciers depend on their material, glacial moraine and snow and ice compositions. The proportions of glacial moraines, especially surface debris, and snow depth on glaciers affect their spectral features. Methods using optical remote sensing (e.g., NDSI method) can only identify relatively clean glacier but not debris-covered glacier (Shukla *et al*., 2010). The spectral information for this debris is similar to that of the bare rocks around the glacier. Thus, these debris-covered glaciers are difficult to distinguish, and this problem affects glacier boundary extraction. However, the surface temperature of debris is lower than that of the surrounding objects due to the underlying glacier (Bhambri *et al*., 2011; Karimi *et al*., 2012). Therefore, the surface temperature can be used to identify debris-covered glacier (Paul *et al*., 2004; Lambrecht *et al*., 2011). Remote sensing images with improved spatial resolution, and surface temperature extracted from thermal infrared image in the support of other auxiliary data such as the digital elevation model (DEM) can be used to more accurately extract debris-covered glacier boundaries (Bhambri *et al*., 2011). Brenning *et al*. (2012) used day and night ASTER images to measure the near-surface temperature to extract the boundaries of the debris-covered glaciers, and the reuslt showed that the surface temperature of the Chilean Andes debris-covered glacier was significantly lower than that of the surrounding rocks and vegetation. This finding indicated that the method could effectively identify debris-covered glaciers when combined with optical and thermal infrared images. Shukla *et al*. (2010) used IRS-P6-AWiFS and TERRA-ASTER optical and thermal infrared images to map the boundaries of the Samudra Tapub glacier, and the result indicated that this method was suitable and very accurate for the identification of debris-covered glaciers.

Therefore, the free optical and thermal infrared images of Landsat are used to extract the boundaries of debris-covered glaciers in the Yigong Zangbo basin, and our study aims to improve the accuracy of glacier identification and to analyze dynamic glacier changes between 1990 and 2015. The impacts of the glacier change on moraine lakes are examined, and one of impact factors of glacier change, air temperature, is explored as well.

2. Study area

The study area is a sub-watershed of the Yigong Zangbo basin (94°32′ - 95°12′E, 30°15′ - 30°38′N) in the eastern region of the Nyainqentanglha mountains and at the eastern end of the Himalayas. This area is under the administration of Bomi County, Tibet Autonomous Region (Fig. 1). The area is 1,662 km^2 and the elevation of the terrain is high in the north and low in the south with an altitude of 2,200 to 6,500 m. The terrain is characterized by high mountains and deep valleys and is dotted with numerous glaciers and snow-capped mountains. Yigong Zangbo River is a tributary of the Brahmaputra River. There is the largest group of glaciers in the Tibetan Plateau. Qiaqing glacier, one of China's three major glaciers and China's largest temperate-glacier, is located in the Yigong Town of Bomi County. Southwest monsoon from the Indian Ocean brings plenty of precipitation, consequently, temperate-glaciers form in this area (Shi and Liu, 2000). The moisture-laden warm air current from the Indian Ocean enters the Yigong Zangbo valley along the Brahmaputra River and results in an apparent altitudinal climatic zonation from the bottom of the valley to the ridge of the watershed. The climate is subtropical under 2700 m, warm and semi-humid highland at 2700-4200 m, and cold and wet temperate highland above 4200 m. The records of Bomi station,

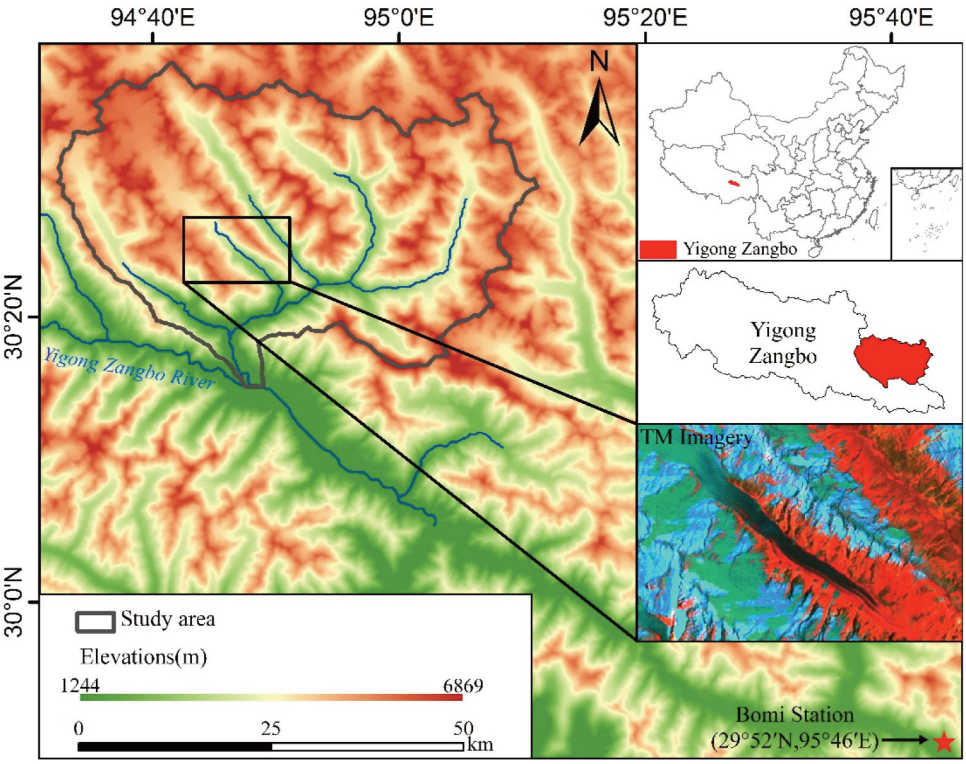

Fig. 1. The location of Yigong Zangbo basin, overlying SRTM DEM.

the closest meteorological station to the study area, show that annual mean air temperature in the Yigong Zangbo basin is 8.5°C, with a mean air temperature of 17.2°C in July and -1.7°C in January, and annual mean precipitation is 958 mm.

As a sub-watershed, the study area accounts for 12.3% of the Yigong Zangbo basin (Fig. 1). According to records from the Global Land Ice Measurements from Space (GLIMS) (https://www.glims.org/), there are 207 glaciers in the study area, with most glaciers situated at an altitude of more than 3500 m. On the one hand, seasonal changes of temperature and precipitation in this basin are significant so that glacier melt is very evident and the equilibrium line is low (Yao *et al*., 2010). On the other hand, glaciers in the Yigong Zangbo basin are affected by warm and humid airflow from the Indian Ocean, these glaciers flow rapidly and have active glacial processes, and are extremely sensitive to global warming (Ke *et al*., 2013). Thus, it is necessary to examine glacier change in the Yigong Zangbo basin.

3. Data and methods

1) Data

Generally, the most significant snowmelt occurs in summer. Therefore, it is the least interference for glacier identification and remote sensing images selected from this period can improve the accuracy of glacier boundary extraction (Xu *et al*., 2013). However, due to cloudy weather and coarse temporal resolution, it is difficult to find suitable Landsat images in the same season, especially in summer. Here, Themetic Mapper (TM) images of Landsat5 (Path 135-Row 39) in 1990 and 2000, as well as Operational Land Imager (OLI) and Thermal Infrared Sensor (TIRS) of Landsat8 (Path 135-Row 39) in 2015 (Table 1), downloaded from the United States Geological Survey (USGS) (https://earthexplorer.usgs.gov/), are used for glacier identification and change analysis in the study area. TM images in 1990 and 2000 are in spring, but May is last month of spring, and glacier condition is close to that in summer, therefore, in our opinion, the images can be used for glacier change comparison with that of Landsat 8 in July 2015. Certainly, we have no other choice but to use them because of cloudy weather.

The Shuttle Radar Topography Mission (SRTM) has a resolution of 90 m, and this resolution can be improved to 30 m by smoothing with 11 * 11 Neighborhood Statistics and resampling. The processed DEM data are used to extract the boundaries of the study area, and to analyze changes in the glacier terminus elevation. The temperature data of Bomi meteorological station (1961-2015), obtained from the National Meteorological Information Center of China, are used to analyze the impacts of temperature changes on glaciers. The CGI and GLIMS database are used to obtain basic information of glaciers, for example, international uniformed name and code of glaciers, and also used as references to validate and correct the classification results.

2) Data preprocessing

All bands of TM and OLI/TIRS are calibrated, and atmospheric correction is performed with Fast Line-of-sight Atmospheric Analysis of Spectral Hypercubes (FLAASH), and topographic correction is implemented

Table 1. Information for Landsat images used in this study

Sensor	Date (dd-mm-yyyy)	Resolutions for optical/thermal bands (m)	Cloud cover
Landsat TM	17-5-1990	30/120	3.0%
Landsat TM	12-5-2000	30/120	1.0%
Landsat OLI/TIRS	25-7-2015	30/100	5.5%

with the improved C modification method (Huang *et al*., 2005). The brightness temperature obtained from the thermal bands is resampled to a resolution of 30 m in order to match the optical band resolution. In addition, the brightness temperature data are normalized. All data are converted to the same projection (WGS 1984, UTM 47N), and cropped with vector boundary of the study area.

3) Classification

For debris-covered glaciers, the pre-processed images are classified using the spectral reflectance of optical bands and the brightness temperature of thermal infrared bands (Fig. 2). Because optical characteristics and the thermal infrared radiation values of illuminated areas differ from those of the shaded areas, the images are divided into illuminated and shaded areas according to D values calculated with formula (1) (Shukla *et al*., 2010).

$$D = \varphi - A \tag{1}$$

where φ is the sun azimuth at the time of image acquisition and A is the aspect angle derived from the DEM. When D is in the range of [-90°, 90º], covering area of the image is an illuminated area at that time, otherwise in a shaded area. The classified types include clean glacier, debris-covered glacier, moraine lake and non-glacier area. The training samples are selected on the basis of the ground object characteristics of the optical band and the temperature characteristics of the thermal band. For the illuminated areas of the images, training samples for the optical band and thermal band are selected for each class, respectively. For the shaded areas, training samples are selected with the same method as the illuminated areas. Table 2 shows us the detail information of training samples for each class. The illuminated and shaded areas are classified with the maximum likelihood classification (MLC) method, respectively. In addition, the DEM data are used to facilitate classification and interpretation. Finally, the areas classified as illuminated or shaded are merged to complete the classification.

Due to distinguishing snow and glacier difficultly in the thermal infrared and optical bands if there is snow

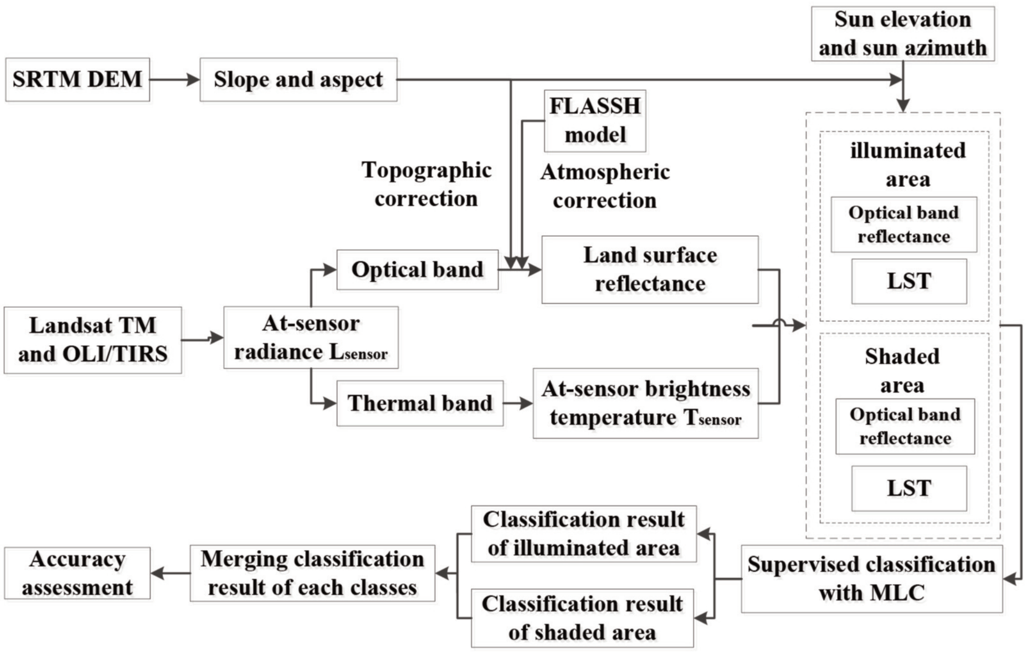

Fig. 2. Glacier identification method based on optical and thermal infrared bands of Landsat TM and OLI/TIRS.

Table 2. The number of classification samples in the illuminated and shaded areas of the images

Classified type	Illuminated area		Shaded area	
	Optical band	Thermal band	Optical band	Thermal band
Clean glacier	40	40	30	30
Debris-covered glacier	25	25	18	18
Moraine lake	6	6	3	3
Non-glacier area	32	32	26	26

in the study area in May and July, a semi-automatic post correction is performed on the classification results by visual interpretation and referring to the CGI and GLIMS database (https://www.glims.org/). SRTM DEM was used to extract mountain ridges, then the boundary of each glacier was quantitatively defined. The images in 1990, 2000 and 2015 are classified using this method to obtain glacier boundaries and to distinguish clean glacier from debris-covered glacier, and our final result is close to the two glacier inventories. Next, statistical analyses of glacier area, moraine lake area, typical glacier length and glacier terminus elevation are carried out.

4) Accuracy assessment

In order to evaluate the accuracy of the classified results derived from remote sensing images covering the study area, we selected 20 same glaciers (about 10% of total glaciers) from the images in 1990, 2000 and 2015. For considering all kinds of conditions for glacier presence as much as possible and their representativeness of samples, these selected glaciers have different size, shape, average elevation, aspect, etc., moreover, some of them are debris-covered glaciers. Then, glacier experts with field experiences and remote sensing knowledge identified these glaciers on the images by visual interpretation, and this interpreted result can be regarded as the 'true values' for accuracy assessment of the classified results. The overall accuracies of the classified results in 1990, 2000 and 2015 were found to be 92.4%, 89.6% and 94.1%, respectively. On the one hand, snow is a possible impact factor for errors. It is difficult to distinguish snow and glacier because of similar spectral features. Particularly, images in 1990 and 2000 are in May, and there is possible snow cover at this time, their accuracies are therefore lower than that of images in July 2015. On the other hand, debris is also a possible impact factor for errors. If debris on a glacier is too thick, thermal remote sensing can not accurately identify the underlying glacier because of little or no surface temperature difference between debris and other surrounding objects (Brenning *et al*., 2012). Consequently, field validation is needed to reduce the error and improve the identification of debris-covered glacier.

4. Results

The final classified results are shown in Fig. 3. Glacier areas in 1990, 2000 and 2015 were 928.76 km^2, 918.46 km^2 and 901.51 km^2 (Table 3), respectively. The total glacier area decreased by 27.25 km^2 over 25 years, and this indicated that glacier retreat is very evident in the Yigong Zangbo basin. However, the debris-covered glacier area slightly increased, and their areas in 1990, 2000 and 2015 were 63.39 km^2, 66.24 km^2 and 71.16 km^2, respectively. The debris-covered glaciers are mostly located at the glacier tongues and sides (Fig. 3), and debris is resulted from freeze-thaw action of rocks under global warming, which can prevent glacier from melting to a certain extent (Vincent *et al*., 2016).

In an average condition, the rate of glacier retreat

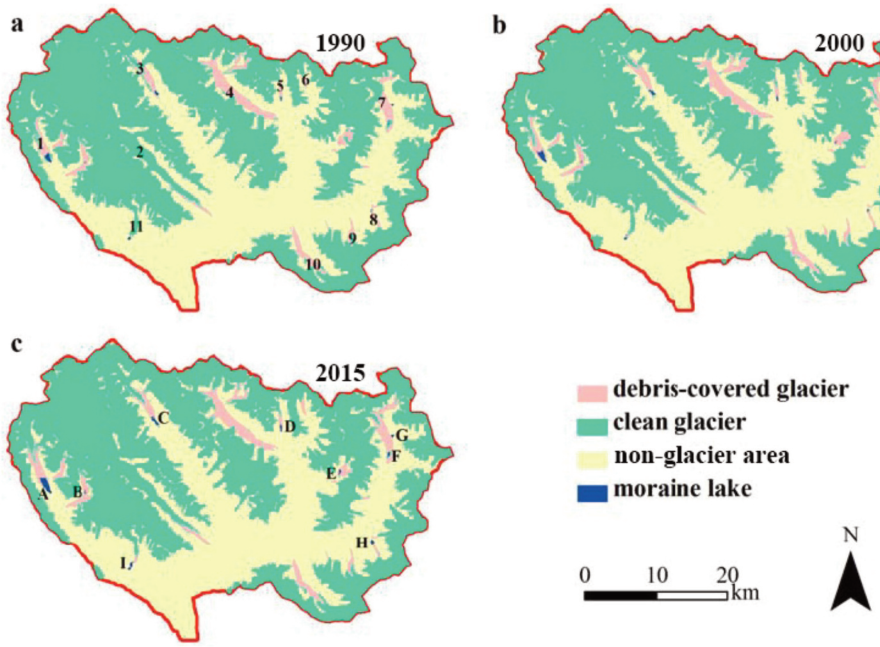

Fig. 3. Glacier and moraine lake distribution in the Yigong Zangbo basin in 1990, 2000 and 2015, 1-11 (figure a) denote index number of measurable glacier (Table 5), and A-I (figure c) denote index number of moraine lake (Table 6).

was 1.09 km^2 yr^{-1} between 1990 and 2015 (Table 4). The glacier area decreased by 10.30 km^2 with a retreat rate of 1.03 km^2 yr^{-1} from 1990 to 2000, and it decreased by 16.95 km^2 from 2000 to 2015 with a retreat rate of 1.13 km^2 yr^{-1}. The retreat rate increased by 9.71% between 2000 and 2015 relative to that occurred between 1990 and 2000. The glacier shrinkage in the southeastern Tibetan Plateau (such as Yigong Zangbo basin) was the most pronounced in the entire Tibetan Plateau, and it also shows accelerating since 2000 (Azam *et al*., 2018; Yao *et al*., 2012).

Within 11 large glaciers examined (Table 5), the largest glacier 5O281B0729 (Gongpu) retreated from 186.53 km^2 in 1990 to 182.03 km^2 in 2000 and 181.17 km^2 in 2015, its length shortened 665 m from 1990 to 2015, and its terminus elevation of ice tongue risen from 2777 m in 1990 to 2911 m in 2015. Meanwhile, the glacier 5O281B0768 (Nalong) showed the most

Table 3. Glacier areas in the Yigong Zangbo basin in 1990, 2000 and 2015 (unit: km^2)

Year	Area of clean glacier	Area of debris-covered glacier	Sum
1990	865.37	63.39	928.76
2000	852.22	66.24	918.46
2015	830.35	71.16	901.51

Table 4. Area and rate of glacier retreat in the Yigong Zangbo basin from 1990 to 2015

Period	Area of glacier retreat (unit: km^2)	Rate of glacier retreat (km^2 yr^{-1})
2000-1990	-10.30	-1.03
2015-2000	-16.95	-1.13
2015-1990	-27.25	-1.09

Table 5. Measurable glacier area, length and terminus elevation in the Yigong Zangbo basin from 1990 to 2015

No.	Glacier	1990			2000-1990		2000	2015-2000		2015
		Area (km^2)	Length (m)	Terminus elevation (m)	Area change (%)	Length change (m)	Terminus elevation (m)	Area change (%)	Length change (m)	Terminus elevation (m)
1	5O281B0714 (Daoge)	64.62	13904	4077	-2.03	-487	4098	-2.13	-1598	4121
2	5O281B0729 (Gongpu)	186.53	34928	2777	-2.41	-243	2857	-0.47	-422	2911
3	5O281B0746 (Ruoguo)	66.03	13977	3655	-1.13	-217	3773	-1.50	-1948	3863
4	5O281B0768 (Nalong)	107.89	18182	3461	-3.37	-353	3566	-2.56	-297	3630
5	5O281B0776	14.75	7368	3951	-0.66	-50	3962	-0.27	-337	4037
6	5O281B0786	6.47	5562	4516	-0.25	-547	4532	-0.09	-493	4592
7	5O281B0813 (Maguolong)	63.33	14790	4057	-1.28	-82	4094	-1.18	-14	4136
8	5O281B0840	13.93	5729	4163	-0.51	-70	4173	-0.33	-301	4198
9	5O281B0842	13.45	6763	3888	-0.73	-88	3901	-0.13	-87	3904
10	5O281B0849 (Yangbiegong)	46.41	15305	3129	-0.21	-215	3210	-1.76	-592	3248
11	5O281B0720 (Qiaqing)	33.63	12190	2695	-1.57	-49	2703	-0.88	-679	2777

significant area reduction of 3.37% from 1990 to 2000 and 2.56% from 2000 to 2015. All glaciers had the same trend, their areas reduced, resulting in shorter lengths and higher terminus elevations. This is consistent with the overall trends for glacier retreat in the Tibetan Plateau (Brun *et al*., 2017). Liu *et al*. (2005) drew a similar conclusion and indicated that glaciers in the southeastern Tibetan Plateau retreated faster after 1980 due to global warming.

The classified results of images showed that moraine lakes emerged at the glacier terminus and gradually increased in size (Fig. 3), and 9 moraine lakes exist in

Table 6. Changes in area of moraine lakes in the Yigong Zangbo basin from1990 to 2015 (unit: km^2)

ID	1990	2000-1990		2000	2015-2000		2015
	Area	Area change	Percentage (%)	Area	Area change	Percentage (%)	Area
A	0.69	0.33	48	1.02	0.59	58	1.61
B	0.03	0.01	33	0.04	0.04	100	0.08
C	0.21	0.07	33	0.28	0.23	82	0.51
D	0.10	0.03	30	0.13	0.08	62	0.21
E	0.01	0.04	400	0.05	0.10	200	0.15
F	0.09	0.03	22	0.11	0.04	36	0.15
G	0.08	0.01	13	0.09	0.04	44	0.13
H	0.09	0.03	33	0.12	0.12	100	0.24
I	0.13	0.01	8	0.14	0.19	136	0.33
Sum	1.43	0.55	38	1.98	1.43	72	3.41

the study area (Table 6). The total area of these moraine lakes was 1.43 km^2 in 1990 and increased by 38% (0.55 km^2) in 2000, and it was 3.41 km^2 in 2015, which was 2.38 times of its area in 1990. The area of the largest moraine lake A increased from 0.69 km^2 in 1990 to 1.61 km^2 in 2015. The area of moraine lake E in 2000 was 4.00 times of that in 1990, and expanded to 0.15 km^2 in 2015, which is 15.00 times of that in 1990.

5. Discussion

All moraine lakes mainly expanded towards the glacier terminus, the glacier terminus retreated and its location was eventually occupied by the moraine lake (Fig. 3). The accelerated expansion of the moraine lake area after 2000 indirectly indicates the accelerated melting and retreat of the glaciers. Che *et al*. (2014) demonstrated that glacial lakes of the Pumqu River basin in the Tibetan Plateau expanded faster in the period of 2001-2013 than in the period of 1970s-2000. This is verified by our present study in the Yigong Zangbo basin. Due to global warming, the moraines formed depressions and blocked the rivers as the glaciers retreated, which resulted in a moraine lake at the glacier terminus and caused the area to expand gradually, and the increasing number and area of moraine lakes became more widespread in the Tibetan Plateau after 2000 (Veh *et al*., 2018). In addition, outburst floods of moraine lakes often occurred and threatened downstream residents (Harrison *et al*., 2018), therefore, monitoring moraine lake area expansion due to glacier retreat is important for preventing such disasters. Knowledge regarding the expansion of moraine lakes can provide a basis for making decisions to prevent moraine lake outburst and ensure the safety of residents living in the downstream.

The analysis of data from Bomi station indicates an overall increasing trend in air temperature of the Yigong Zangbo basin from 1961 to 2015 (Fig. 4), with a growth rate of approximately 0.325 °C/decade. The air temperature increased significantly faster between 1990 and 2015, with +0.603 °C/decade. The rapid air temperature rise in the recent decades enhanced freeze-thaw action, leading to more debris covering on glaciers and increase in area of debris-covered glaciers (Lambrecht *et al*., 2011). On the other hand, the rapid air temperature rise could have been the main reason for the glacier retreat, which resulted in moraine lake expansion. The study by Shi and Liu (2000) also indicated that maritime glaciers had poor sensitivity to changes in precipitation, however, increasing temperatures significantly impacted changes in maritime glaciers and accelerated glacier melting.

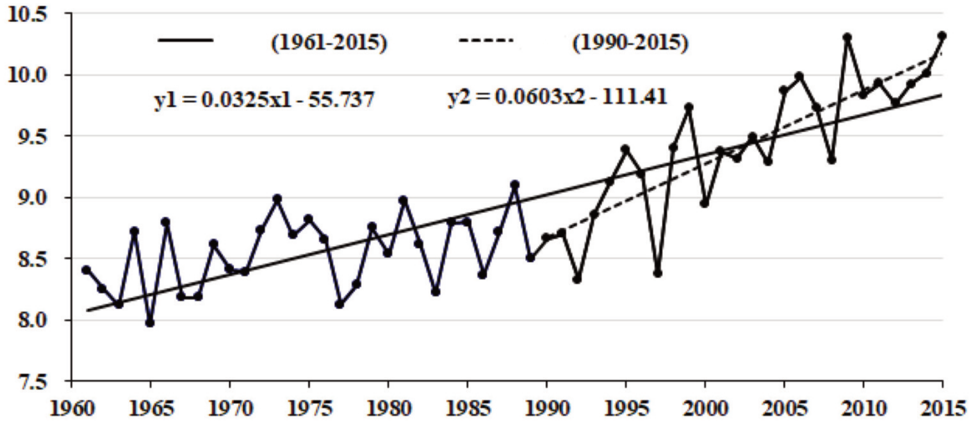

Fig. 4. Change in annual mean air temperature (°C) at Bomi meteorological station from 1961 to 2015.

6. Conclusions

The optical and thermal infrared band images of Landsat in 1990, 2000 and 2015 are used to identify and extract the glacier boundaries in the Yigong Zangbo basin. These measurements are based on the surface temperature differences among the clean glaciers, debris-covered glaciers and surrounding objects. Changes in the glacier area, length and terminus elevation are analyzed. In addition, changes in the moraine lake areas and the impacts of temperature rise on glaciers are further discussed.

Overall, the glaciers were receding and melting, with an area reduction of 27.25 km^2 over 25 years. However, the debris-covered glacier area slightly increased, and their areas in 1990, 2000 and 2015 were 63.39 km^2, 66.24 km^2 and 71.16 km^2, respectively. In an average condition, the glaciers retreated at a rate of 1.03 $km^2\ yr^{-1}$ between 1990 and 2000, at a rate of 1.13 $km^2\ yr^{-1}$ between 2000 and 2015. The glaciers generally became shorter, and the terminus elevations of the glacier tongues risen. The total area of the moraine lakes was 1.43 km^2 in 1990 and 1.98 km^2 in 2000. The moraine lakes expanded drastically after 2000, reaching 3.41 km^2 in 2015 (2.38 times of its area in 1990). The annual mean air temperature risen significantly from 1961 to 2015, and the greater air temperature increase accelerated the glacier retreat after 1990.

The data for glacier identification, especially for the parameters of the debris-covered glaciers on complex terrains, are obtained through the classification of optical and thermal bands of Landsat images. These data can be used as a supplement to the glacier inventory. Even in summer, the interference of snow in the high elevation areas could not be eliminated completely due to the similar spectral features of snow and glacier. In addition, thick debris is also an impact factor, and results in certain error occurrence in the glacier identification. Therefore, high-resolution SAR image should be used to overcome these drawbacks to obtain more accurate identification information of debris-covered glacier in the future study (Huang *et al*., 2018).

Acknowledgements

This research was supported by the National Nature Science Foundation of China (No. 41830105) and also funded by the International Scholar Exchange Fellowship (ISEF) program at KFAS (Korean Foundation of Advanced Studies). The Landsat data are obtained from the United States Geological Survey (USGS) (https://earthexplorer.usgs.gov/).

References

Azam, M.F., P. Wagnon, E. Berthier, C. Vincent, K. Fujita, and J.S. Kargel, 2018. Review of the status and mass changes of Himalayan-Karakoram glaciers, *Journal of Glaciology*, 64(243): 61-74.

Bhambri, R., T. Bolch, and R.K. Chaujar, 2011. Mapping of debris-covered glaciers in the Garhwal Himalayas using ASTER DEMs and thermal data, *International Journal of Remote Sensing*, 32(23): 8095-8119.

Brenning, A, M.A. Peña, S. Long, and A. Soliman, 2012. Thermal remote sensing of ice-debris landforms using ASTER: an example from the Chilean Andes, *The Cryosphere*, 6(2): 367-382.

Brun, F., E. Berthier, P. Wagnon, A. Kääb, and D. Treichler, 2017. A spatially resolved estimate of High Mountain Asia glacier mass balances from 2000 to 2016, *Nature Geoscience*, 10(9): 668-674.

Che, T., L. Xiao, and Y.A. Liu, 2014. Changes in glaciers and glacial lakes and the identification of dangerous glacial lakes in the Pumqu River basin, Xizang (Tibet), *Advances in Meteorology*, 2014: 1-8.

Collier, E., F. Maussion, L.I. Nicholson, T. Mölg, W.W. Immerzeel, and A.B.G. Bush, 2015. Impact of debris cover on glacier ablation and atmosphere-glacier feedbacks in the Karakoram, *The Cryosphere*, 9: 1617-1632.

Huang, L., Z. Li, H. Han, B.S. Tian, and J.M. Zhou, 2018. Analysis of thickness changes and the associated driving factors on a debriscovered glacier in the Tienshan Mountain, *Remote Sensing of Environment*, 206: 63-71.

Huang, W., L.P. Zhang, and P.X. Li, 2005. An improved topographic correction approach for satellite image, *Journal of Image and Graphics*, 10: 1124-1128 (in Chinese).

Karimi, N., A. Farokhnia, L. Karimi, M. Eftekhari, and H. Ghalkhani, 2012. Combining optical and thermal remote sensing data for mapping debris-covered glaciers (Alamkouh Glaciers, Iran), *Cold Regions Science and Technology*, 71: 73-83.

Ke, C.Q., C. Kou, R. Ludwig, and X. Qin, 2013. Glacier velocity measurements in the eastern Yigong Zangbo basin, Tibet, China, *Journal of Glaciology*, 59(218): 1060-1068.

Lambrecht, A., C. Mayer, W. Hagg, V. Popovnin, and A. Rezepkin, 2011. A comparison of glacier melt on debris-covered glaciers in the northern and southern Caucasus, *The Cryosphere*, 5: 525-538.

Li, B., X. Li, and X.Z. Chen, 1999. The design of the management system of Chinese Glacier Inventory, *Journal of Glaciology and Geocryology*, 21: 77-80 (in Chinese).

Liu, C.H., Y.F. Shi, Z.T. Wang, and Z.C. Xie, 2000. Glacier resources and their distributive characteristics in China-A review on Chinese glacier inventory, *Acta Geographica Sinica*, 22: 106-112.

Harrison, S., J.S. Kargel, C. Huggel, J. Reynolds, D.H. Shugar, R.A. Betts, A. Emmer, N. Glasser, U.K. Haritashya, J. Klimeš, L. Reinhardt, Y. Schaub, A. Wiltshire, D. Regmi, and V. Vilímek, 2018. Climate change and the global pattern of moraine-dammed glacial lake outburst floods, *The Cryosphere*, 12: 1195-1209.

Liu, S., D.H. Shangguan, Y.J. Ding, H.D. Han, and Y. Zhang, 2005. Glacier variations since the early 20th century in the Gangrigabu Range, Southeast Tibetan Plateau, *Journal of Glaciology and Geocryology*, 27(1): 55-63 (in Chinese).

Liu, S.Y., N.L.Wang, Y.J. Ding, and Z.C. Xie, 1999. On the characteristics of glacier fluctuation during the last 30 years in Urumqi River Basin and the estimation of temperature rise in the high mountain area, *Advances in Earth Science*, 14: 279-285 (in Chinese).

Paul, F., C. Huggel, and A. K??b, 2004. Combining satellite multispectral image data and a digital elevation model for mapping debris-covered glaciers, *Remote Sensing of Environment*, 89(4): 510-518.

Scherler, D., H. Wulf, and N. Gorelick, 2018. Global assessment of supraglacial debris-cover extents, *Geophysical Research Letters*, 45(21): 11798-11805.

Shangguan, D.H., S.Y. Liu, Y.J. Ding, L.F. Ding, and G. Li, 2004. Glacier changes at the head of Yurungkax River in the west Kunlun Mountains in the past 32 years, *Acta Geographica Sinica*, 59(6): 855-862.

Shi, Y.F. and S.Y. Liu, 2000. Estimation on the response of glaciers in China to the global warming in the 21st century, *Chinese Science Bulletin*, 45(7): 668-672.

Shukla, A., M.K. Arora, and R.P. Gupta, 2010. Synergistic approach for mapping debris-covered glaciers using optical-thermal remote sensing data with inputs from geomorphometric parameters, *Remote Sensing of Environment*, 114(7): 1378-1387.

Veh, G., O. Korup, S. Roessner, and A. Walz, 2018. Detecting Himalayan glacial lake outburst floods from Landsat time series, *Remote Sensing of Environment*, 207: 84-97.

Vincent, C., P. Wagnon, J.M. Shea, W.W. Immerzeel, P. Kraaijenbrink, D. Shrestha, A. Soruco, Y. Arnaud, F. Brun, E. Berthier, and S.F. Sherpa, 2016. Reduced melt on debris-covered glaciers: investigations from Changri Nup Glacier, Nepal, *The Cryosphere*, 10: 1845-1858.

Xu, J.L., S.Y. Liu, S.Q. Zhang, W.Q. Guo, and J. Wang, 2013. Recent changes in glacial area and volume on Tuanjiefeng peak region of Qilian Mountains, China, *PLOS ONE*, 8(8): e70574.

Yan, L.L. and J. Wang, 2013. Study of extracting glacier information from remote sensing, *Journal of Glaciology and Geocryology*, 35(1): 110-118 (in Chinese).

Yao, T.D., Z.G. Li, W. Yang, X.J. Guo, and L.P. Zhu, 2010. Glacial distribution and mass balance in the Yarlung Zangbo River and its influence on lakes, *Chinese Science Bulletin*, 55(20): 2072-2078.

Yao, T.D., L. Thompson, W. Yang, W.S. Yu, and Y. Gao, 2012. Different glacier status with atmospheric circulations in Tibetan Plateau and surroundings, *Nature Climate Change*, 2(9): 663-667.

Zhou,Y., Z. Li,, J. Li, R. Zhao, and X. Ding, 2018. Glacier mass balance in the Qinghai-Tibet Plateau and its surroundings from the mid-1970s to 2000 based on Hexagon KH-9 and SRTM DEMs, *Remote Sensing of Environment*, 210: 96-112.